Extended Abstracts of the 2015 International Conference on Solid State Devices and Materials, Sapporo, 2015, pp918-919

Gigahertz Single-Electron Pump Towards a Representation of the New Ampere

Akira Fujiwara, Gento Yamahata and Katsuhiko Nishiguchi

NTT Basic Research Laboratories, NTT Corporation
3-1, Wakamiya, Morinosato, Atsugi, Kanagawa 243-0198, Japan
Phone: +81-46-240-2643 E-mail: fujiwara.akira@lab.ntt.co.jp

Abstract

A high-speed single-electron (SE) pump is attracting much interest in its application to quantum current standards in terms of redefining the ampere with a fixed-value elementary charge. Here we report on gigahertz SE pumps employing Si nanowire transistors and describe the present status of the accuracy of high-speed SE pumps.

1. Introduction

A single-electron (SE) pump enables one-by-one control of electric charges based on clocked transfer. Recently, realization of the SE-pump-based current standard has been gaining interest in terms redefining the SI base unit ampere [1]. An important milestone is to close the so called quantum metrology triangle (Fig. 1) by which one can confirm the consistency of the SE pump, the Josephson voltage standard, and the quantum Hall resistance standard. This imposes two requirements: (i) the pump current $I = nef$ (n: integer, e: elementary charge, f: clock frequency) must be higher than sub-nanoampere level, thereby requiring f in a gigahertz regime, (ii) the pump accuracy must be high with an error rate below 0.01 ppm.

2. Tunable-Barrier SE Pump

A promising category for high-speed SE pumps is the tunable-barrier SE pump [2]. This device consists of a nanowire or a narrow semiconductor channel with an array of fine gates that form electrostatic barriers in the channel and thereby define a charge island or a quantum dot between the gates. Over the last decade, there have been intensive studies using Si nanowires [3, 4] and GaAs narrow channels [5-7]. Figure 2 (a) shows the top view of such a device using a Si nanowire with fine gates fabricated using electron beam lithography and dry etching. In addition to the fine gates, a wide upper gate is used as a mask for ion implantation to form an n-type or p-type source and drain. The upper gate voltage (V_{UG}) is used to control the potential of the charge island. As shown in Fig. 2 (b), SEs are pumped by applying an AC clock signal to one of the fine gates to tune the height of the potential barrier underneath it and thereby capture and emit SEs, while a constant negative bias is applied to another fine gate to form a fixed barrier. Figures 3(a) and 3(b) show the operations of a tunable-barrier SE pump [4] and a single-hole (SH) pump [8]. SEs and SHs are successfully pumped at gigahertz frequencies via a charge island whose charging energy is in the order of 10 meV.

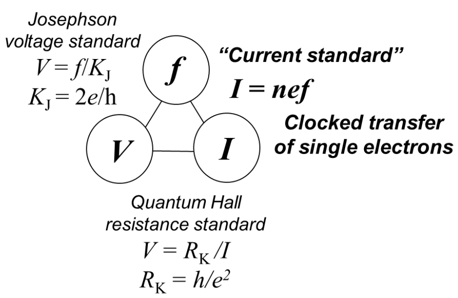

Fig. 1. Quantum metrology triangle.

3. SE Pump Using Localized States

An alternative approach for SE pumps is the use of localized states such as impurity states [9-11] or trap states [12] in Si. This is because we can store a SE in a localized state with a high activation energy. Recently, gigahertz operations of this type of device have been demonstrated using a single dopant [13] and a charge trap [14] in Si.

Figure 2(c) shows the operating principle of the SE pump using a trap [14]. An electron stored in the trap can be emitted by a gate electric field. The trap is most likely ascribed to an interface state since the Si channel is undoped. To find suitable devices containing a single trap at proper locations, we performed a screening test of many devices fabricated on a 4-inch wafer and found several devices operating correctly.

Figure 4 (a) shows typical pump current characteristics of the device containing a trap. A wide current plateau due to the trap-mediated SE pump is obtained in addition to island-mediated ones. Figure 4 (b) shows the trap-mediated SE pump at f =3.5 GHz, indicating that the gate electric field at the trap can emit a trapped electron within a few tens of picoseconds. We investigated the temperature

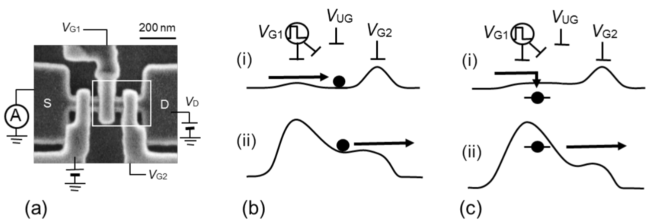

Fig. 2. (a) Top view of an SE pump employing a Si nanowire. The upper gate covers a wide region and is not shown in the figure. Schematic potential diagrams of tunable-barrier SE pumps using (b) a charge island [4] and (c) a localized state [14].

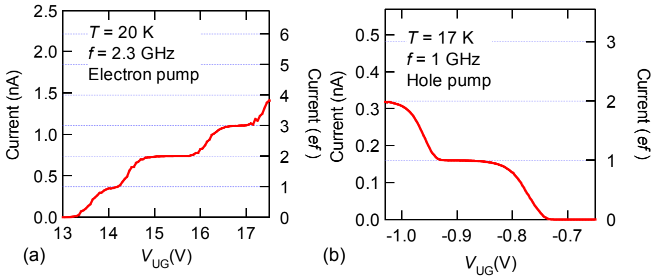

Fig. 3. GHz operations of (a) an SE pump [4] and (b) an SH pump [8].

dependence of the pump currents for two different devices and estimated the effective activation energy of the trap for each device to be 13 and 37 meV.

4. Accuracy of High-Speed SE Pump

The present status of the accuracy of high-speed SE pumps reported so far is summarized in Table. I. Two kinds of methods are employed to measure the accuracy. One is the absolute evaluation of the accuracy by error counting using a charge sensor with SE resolution [12, 15, 16]. The other is a comparison between the pump current and that produced by conventional electrical apparatus traceable to the primary voltage and resistance standards [17-21], in which the uncertainty of the measurement can reach the ppm [17] or sub-ppm [20] level. With this method, accuracy of the SE pumps at the 1 ppm [17, 19, 21] or 0.2 ppm [20] has been confirmed. For island-mediated SE pumps, the best-case accuracy is also estimated by fitting the measured shape of the current plateaus to the so-called decay cascade model [22] based on non-equilibrium electron capture to a charge island [4]. Many studies have suggested the possibility of accuracy at 0.01 ppm level [14, 16-18, 21, 23], which is expected to be experimentally proven in the near future.

5. Conclusions

Tunable-barrier SE pumps with a charge island or a localized state are promising for electrical current standards towards a representation of the new ampere.

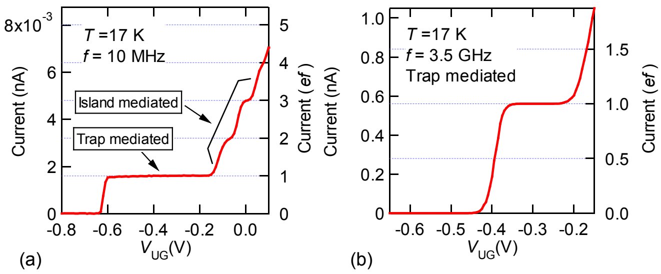

Fig. 4. (a) Pump characteristics of the device containing a charge trap. (b) Operation of the trap-mediated SE pump at 3.5 GHz [14].

Acknowledgements

We thank T. Karasawa for his help with device characterization. This work was partly supported by the Funding Program for Next Generation World-Leading Researchers of JSPS (GR 103).

References

[1] J. P. Pekola et al., Rev. Mod. Phys. **85** (2013) 1421.
[2] B. Kaestner and V. Kashcheyevs, arXiv:1412.7150 (2014).
[3] A. Fujiwara et al., Appl. Phys. Lett. **84** (2004) 1323.
[4] A. Fujiwara et al ., Appl. Phys. Lett. **92** (2008) 042102.
[5] M. D. Blumenthal et al., Nature Phys. **3** (2007) 343.
[6] B. Kaestner et al., Phys. Rev. B **77** (2008) 153301.
[7] B. Kaestner et al., Appl. Phys. Lett. **94** (2009) 012106.
[8] G. Yamahata et al., Appl. Phys. Lett. **106** (2015) 023112.
[9] D. Moraru et al., Phys. Rev. B **76** (2007) 075332.
[10] G. P. Lansbergen et al., Nano Lett. **12** (2012) 763.
[11] B. Roche et al., Nat. Commun. **4** (2013) 1581.
[12] G. Yamahata et al., Appl. Phys. Lett. **98** (2011) 222104.
[13] G. C. Tettamanzi et al., New J. Phys. **16** (2014) 063036.
[14] G. Yamahata et al., Nat. Commun. **5** (2014) 5038.
[15] L. Fricke et al., Phys. Rev. Lett. **110** (2013) 126803.
[16] G. Yamahata et al., Phys. Rev. B **89** (2014) 165302.
[17] S. P. Giblin et al., Nat. Commun. **3** (930) 2012.
[18] A. Rossi et al., Nano Lett. **14** (2014) 3405.
[19] M. Bae et al., Metologia **52** (2015) 195.
[20] F. Stein et al., arXiv:1506.05965v1 (2015).
[21] G. Yamahata et al., (unpublished).
[22] V. Kashcheyevs and B. Kaestner, Phys. Rev. Lett. **104**, (2010) 186805.
[23] J. Fletcher et al., Phys. Rev. B **86** (2012) 155311.
[24] M. Seo et al., Phys. Rev. B **90** (2014) 085307.

Table I Present Status of Accuracy of High-Speed SE Pumps

	GaAs quantum dot			**Si charge island (quantum dot)**		**Dopant in Si**	**Trap in Si**
Device	NPL	PTB	KRISS	NTT	UNSW	UNSW	NTT
Frequency	3.4 GHz [5]	0.8 GHz [6]	3 GHz [24]	2.3 GHz [4]	0.5 GHz [18]	1 GHz [13]	3.5 GHz [14], 7.4 GHz [21]
Temperature	1.8 K [5] 300 mK [17]	300 mK[6,7] 25 mK [15] 100 mK [20]	4.2 K [24] 300 mK [19]	20 K [4] 30 mK [16] 1~4 K [21]	80 mK [18]	4.2 K [13]	17 K [12, 14] 1~4 K [21]
Measured accuracy a) b) c)	<1.2 ppm b) 0.945 GHz B = 14 T [17]	1% a) 40 MHz [15] 0.2 ppm b) 0.545 GHz B = 16 T [20]	<1.37 ppm b) 0.95 GHz B = 11 T [19]	100 ppm a) 2 ns rise pulse [16] < ~1 ppm b), 1 GHz, B = 0 T < ~1 ppm b), 2 GHz, B = 14 T [21]	<50 ppm b) 0.5 GHz [18]	-	0.21% a) 2 ns rise pulse [12] <0.1 % c), 3.5 GHz [14] 20 ppm b), 6.5 GHz [21]
Estimated accuracy d) e) (Best case)	0.01 ppm d) 0.945 GHz B = 14 T [17, 23]	300 ppm d) 0.5 GHz B = 10 T [7]	0.1 ppm d) 0.5 GH [24]	0.01 ppm d), 10 MHz [16] 0.01 ppm d), 1 GHz [21]	0.02 ppm d) 100 MHz [18]	-	0.01 ppm e) 1 GHz [14]

a) Error counting with a SE-resolution charge sensor b) Comparison to the current traceable to voltage/resistance standards c) Measurement by ammeter
d) Estimated based on curve fitting to the decay cascade model [22]. e) Estimated by considering errors due to missed transitions and thermal leakage.